MOLECULAR PHYSICS, 1985, VOL. 55, NO. 5, 1193–1215

The hard ellipsoid-of-revolution fluid
II. The y-expansion equation of state

by B. M. MULDER
Institute for Theoretical Physics
Rijksuniversiteit, Utrecht, The Netherlands
and D. FRENKEL
Fysisch Laboratorium, Rijksuniversiteit, Utrecht, The Netherlands

(*Received 5 March 1985 ; accepted 25 March 1985*)

The y-expansion as introduced by Barboy and Gelbart is applied to a system of hard ellipsoids-of-revolution. The expansion is truncated after the third order term yielding an approximate theory requiring the second- and third-virial coefficients as inputs. As the third virial coefficient is not known analytically, numerical results are obtained for this quantity. The equation of state is obtained from a free-energy variational calculation. The results are compared with Monte Carlo data taken from the preceding paper in this series. The application of scaled particle theory to the same system is discussed, and shown to have serious shortcomings.

1. INTRODUCTION

The interest in studying convex hard particle liquids is twofold. First of all, experience with simple liquids has shown that the local structure of such a liquid is almost completely determined by the packing effects due to the short range repulsive interactions between the particles. This accounts for the enormous success of theories based on the hard sphere fluid as a reference system onto which long range interactions are added perturbatively [1]. This suggests that the same approach would be fruitful in the study of systems composed of non-spherical molecules whose effective shape is approximated by a convex hard core. Secondly anisotropic excluded volume interactions are seen to provide a mechanism for the appearance of long range orientational order, thereby serving as a possible basis for a realistic theory of the nematic liquid-crystalline phase. This was first exploited by Onsager, who constructed a theory to describe the behaviour of dilute suspensions of very elongated particles [2]. He was able to show that above a certain solute concentration long range orientational order was favoured by the system, the loss in orientational entropy being offset by a gain in translational entropy due to the decrease in excluded volume between the particles. However his theory is only strictly valid in the isotropic phase of a solution of infinitely extended particles of vanishing proper volume.

The general problem therefore is to construct an accurate equation of state for convex, non-spherical, hard particle fluids. The most rigorous approach towards this goal would seem the solution of one of the well-known integral equations for

the pair-distribution functions of liquids, considering the success of the Percus–Yevick equation in the hard sphere case [3, 4]. Unfortunately the lower symmetry of the particles involved greatly increases the complexity of the equations [5]. Especially if one wishes to consider the possibility of orientational order, in which case the one-particle orientational distribution function appears as a new unknown in the equations. A second equation is then needed to couple this distribution function back to one of the pair-functions [6]. In practice more approximative schemes are used.

The most successful to date is the scaled-particle theory (SPT). Based on the original idea for the hard sphere system of Reiss, Frisch and Lebowitz [7], its generalization to nonspherical particles was considered by several workers [8–11]. Its most extensive application was to the hard spherocylinder system in a series of papers by Cotter and Martire [10] and Cotter [12, 13]. Reasonable results are obtained for the equation of state in the isotropic phase for particles of length-to-breadth ratio L/B up to $L/B = 3$, as compared with computer experiments [14–16]. The predictions for the isotropic-to-nematic transition have not been tested so far due to the unavailability of simulation data.

More recently Barboy and Gelbart [17, 18] have proposed a new method to determine the equation of state of hard particle fluids, the so called y-expansion, based on a formally exact reexpansion of the virial series in a new density type variable. It appears to combine the approximative power of SPT, with a lack of the thermodynamic inconsistency problems connected with the latter. The y-expansion was somewhat later independently proposed by Nezbeda *et al.* [19], who were the first to apply it to a fluid of non-spherical particles with a continuous range of orientations. Their results on the spherocylinder system could be compared with the existing simulation data on this system in the isotropic phase for two length-to-breadth ratios.

Our aim is to carry the investigation of the properties of the y-expansion somewhat further, and look at its predictions for the isotropic-to-nematic transition as well as its isotropic-phase equation of state. Furthermore we would like to consider plate-like particles as well as the rod-like shapes investigated so far. To this end we studied a system composed of hard ellipsoids of revolution on which we did extensive simulation experiments as reported in the foregoing paper [20], henceforth referred to as I.

The paper is organized as follows. The y-expansion is introduced in § 2. The necessary expansion coefficients can be expressed in the second and third virial coefficients, the computation of which we discuss in § 3. As an interlude we turn to the application of SPT to the same system in § 4, showing that it has some serious shortcomings when compared to the y-expansion approach. The actual construction of the equation of state from a free-energy variational calculation is discussed in § 5. The results for the isotropic phase and the isotropic-to-nematic transition are given in § 6. Some conclusions are finally drawn in § 7.

2. The y-expansion

The y-expansion is obtained by considering the free-energy in the grand-canonical ensemble as a functional of the one particle distribution function $\rho^{(1)}(j)$, itself a function of the relevant degrees of freedom of a particle, here collectively

denoted by the index j. The functional is given by [21, 22]

$$\beta F[\rho^{(1)}] = \int dj\rho^{(1)}(j)\{\ln \rho^{(1)}(j) - 1 - \Lambda\} - H[\rho^{(1)}]. \tag{2.1}$$

Here Λ is related to the ideal gas properties of the system through the relation

$$\beta\mu^{\mathrm{id}} = \ln \rho - \Lambda. \tag{2.2}$$

The functional $H[\rho^{(1)}]$ is most easily expressed as a sum over diagrams:

$$H[\rho^{(1)}] = \sum \begin{Bmatrix}\text{irreducible, connected diagrams with} \\ \rho^{(1)} \text{ vertices and } f(i,j) \text{ bonds}\end{Bmatrix} \tag{2.3}$$

where $f(i, j) = \exp[-\beta v(i, j)] - 1$ is the Mayer-function, $v(i, j)$ the pair potential.

Now consider a system of non-spherical particles, described by their position $\mathbf{r}_j$ and orientation Ω_j with respect to a fixed reference frame. We shall assume that the system is translationally invariant, but allow for the possibility of orientational order. The one-particle distribution function will then be given by

$$\rho^{(1)}(j) = \rho\psi(\Omega_j), \tag{2.4}$$

where ρ is the number density and $\psi(\Omega_j)$ an orientation-distribution function with unit norm. Introducing this into (2.1) yields

$$\beta F[\psi] = N\left\{\int d\Omega\psi(\Omega) \ln \psi(\Omega) + \ln \rho - 1 - \Lambda + \sum_{n=2}^{\infty} \frac{B_n[\psi]}{(n-1)} \rho^{n-1}\right\}. \tag{2.5}$$

Here we have introduced the virial-coefficients $B_n[\psi]$ defined as

$$B_n[\psi] = -\frac{(n-1)}{V} \sum \begin{Bmatrix}\text{irreducible, connected diagrams with} \\ n\ \psi(\Omega) \text{ vertices and } f \text{ bonds.}\end{Bmatrix}, \tag{2.6}$$

where V is the volume of the system.

The idea of the y-expansion is to replace the expansion in terms of the number density ρ, by an expansion in a new variable y, defined as

$$y = \frac{\rho}{1 - v_0\rho}, \tag{2.7}$$

where v_0 is the hard core volume of the particle. The following relation defines the y-expansion coefficients $C_n[\psi]$:

$$\ln \rho + \sum_{n=2}^{\infty} \frac{B_n[\psi]}{(n-1)} \rho^{n-1} \equiv \ln y + \sum_{n=2}^{\infty} \frac{C_n[\psi]}{(n-1)} y^{n-1}. \tag{2.8}$$

Thus one has

$$C_n[\psi] = (n-1) \sum_{k=2}^{n} \binom{-k+1}{n-k} \frac{B_k[\psi]}{(k-1)} v_0^{n-k} + (-)^{n-1} v_0^{n-1}. \tag{2.9}$$

Other thermodynamic quantities are now easily expressed in terms of the y-expansion. For the pressure one has

$$\beta P = \sum_{n=1}^{\infty} C_n[\psi] y^n, \tag{2.10}$$

where we have defined $C_1(\psi) = 1$. The chemical potential reads as

$$\beta\mu = \int d\Omega\psi(\Omega) \ln \psi(\Omega) - \Lambda + \ln y + \sum_{n=1}^{\infty} \left[\left(1 + \frac{1}{n}\right)C_{n+1} + v_0 C_n\right] y^n. \quad (2.11)$$

The advantage of the y-expansion lies in its assumed convergence properties. This is best illustrated by considering the case of hard spheres and truncating the expansion for the equation of state (2.10) after the third order term. One immediately obtains the well known Percus–Yevick compressibility result, known to agree well with 'experiment' up to crystallisation density. To obtain the same type of agreement from the original virial expansion at least seven terms should be taken into account. In our application we will work with the y-expansion truncated after the third order term. To this end the coefficients $C_2[\psi]$ and $C_3[\psi]$ are needed. Their relation to the traditional virial coefficients is easily obtained from (2.9)

$$C_2[\psi] = B_2[\psi] - v_0, \quad (2.12a)$$

$$C_3[\psi] = B_3[\psi] - 2v_0 B_2[\psi] + v_0^2. \quad (2.12b)$$

3. Evaluation of the expansion coefficients

We now turn to the explicit evaluation of the expansion coefficients $C_2[\psi]$ and $C_3[\psi]$ for the case of hard ellipsoids of revolution. The ellipsoids are characterized by the lengths a and b of their major and minor axes respectively. Their length-to-breadth ratio we define as $x = a/b$. From (2.12) we see that we are faced with the evaluation of the virial-coefficients $B_2[\psi]$ and $B_3[\psi]$.

3.1. *The second virial coefficient*

From its definition (2.6) the second virial coefficient is given by

$$B_2[\psi] = -\frac{1}{2V} \int d\mathbf{r}_1\, d\mathbf{r}_2\, d\hat{\Omega}_1\, d\hat{\Omega}_2\, \psi(\hat{\Omega}_1)\psi(\hat{\Omega}_2) f(\mathbf{r}_1 - \mathbf{r}_2 \hat{\Omega}_1 \hat{\Omega}_2). \quad (3.1.1)$$

Here we have introduced the unit vectors $\hat{\Omega}_j$ along the major axis of the ellipsoids, completely specifying their orientation. Because we are dealing with hard interactions, the integral over the relative positions of the particles simply yields the excluded volume of two ellipsoids with given orientation. We are left with

$$B_2[\psi] = \frac{1}{2} \int d\hat{\Omega}_1\, d\hat{\Omega}_2\, \psi(\hat{\Omega}_1)\psi(\hat{\Omega}_2) E(\hat{\Omega}_1 \cdot \hat{\Omega}_2). \quad (3.1.2)$$

$E(\hat{\Omega}_1 \cdot \hat{\Omega}_2)$ is the excluded volume of two ellipsoids with fixed orientations $\hat{\Omega}_1$ and $\hat{\Omega}_2$. From symmetry we see that it is only a function of the angle between the major axes of the ellipsoids. Isihara [23] has given an explicit expression for this quantity in the form of an expansion in Legendre-polynomials

$$E(\hat{\Omega}_1 \cdot \hat{\Omega}_2) = 2v_0 + \sum_{l=0}^{\infty}{}' \frac{2l+1}{4\pi} \begin{Bmatrix} a_l(x) \\ b_l(x) \end{Bmatrix} P_l(\hat{\Omega}_1 \cdot \hat{\Omega}_2), \quad \begin{matrix} x > 1 \\ x < 1 \end{matrix}. \quad (3.1.3)$$

The prime on the summation indicates that only terms with even value of l contribute, reflecting the inversion symmetry of the ellipsoids with respect to

their centre of mass. The explicit form of the coefficients $a_l(x)$ and $b_l(x)$ is given in appendix A.

An intriguing feature of these coefficients was found when numerically evaluating them for ellipsoids with inverse length-to-breadth ratios. For all cases considered we found

$$\frac{a_l(x)}{v_0(x)} = \frac{b_l(1/x)}{v_0(1/x)}, \qquad x > 1, \tag{3.1.4}$$

where $v_0(x)$ is the volume of the ellipsoid. The relation implies that the pair excluded volume, measured in units of the proper volume, of prolate and oblate ellipsoids, with the same eccentricity, is equal. Isihara already noticed this symmetry for the terms with $l = 0$. In appendix B we give a proof of this property.

3.2. *The third virial coefficient*

We now turn to the third virial coefficient

$$B_3[\psi] \equiv \frac{1}{3} \int d\hat{\Omega}_1 \, d\hat{\Omega}_2 \, d\hat{\Omega}_3 \, K(\hat{\Omega}_1, \hat{\Omega}_2, \hat{\Omega}_3)\psi(\hat{\Omega}_1)\psi(\hat{\Omega}_2)\psi(\hat{\Omega}_3). \tag{3.2.1}$$

Here we have defined the angle dependent kernel

$$K(\hat{\Omega}_1, \hat{\Omega}_2, \hat{\Omega}_3) = -\int d\mathbf{r}_{12} \, d\mathbf{r}_{13} \, f(\mathbf{r}_{12}, \hat{\Omega}_1, \hat{\Omega}_2) f(\mathbf{r}_{13}, \hat{\Omega}_1, \hat{\Omega}_2) f(\mathbf{r}_{23}, \hat{\Omega}_3, \hat{\Omega}_3),$$

where $\mathbf{r}_{ij} = \mathbf{r}_j - \mathbf{r}_i$. The effect of the hard-core Mayer function is to let only simultaneous overlapping configurations of all three particles contribute to the integral. Hence the kernel K can also be interpreted as

$$K(\hat{\Omega}_1\hat{\Omega}_2\hat{\Omega}_3) = V^2 P^3(\hat{\Omega}_1\hat{\Omega}_2\hat{\Omega}_3) = V^2 \cdot \begin{cases} \text{probability of simultaneous overlap} \\ \text{of three particles with fixed} \\ \text{orientations } \hat{\Omega}_k \text{ when randomly} \\ \text{inserted into a volume } V. \end{cases} \tag{3.2.2}$$

This observation allows us to reduce the problem considerably. To this end note that the three-particle probability can be split in the following manner:

$$P^{(3)}(\hat{\Omega}_1, \hat{\Omega}_2, \hat{\Omega}_3) = P^{(2)}(\hat{\Omega}_1, \hat{\Omega}_2)P^{(2)}(\hat{\Omega}_1, \hat{\Omega}_3)P_c^{(3)}(\hat{\Omega}_2, \hat{\Omega}_3 \,|\, (\hat{\Omega}_1, \hat{\Omega}_2)(\hat{\Omega}_1, \hat{\Omega}_3)). \tag{3.2.3}$$

Here $P^{(2)}(\hat{\Omega}_i, \hat{\Omega}_j)$ is the probability of overlap of two particles i and j and $P_c^{(3)}(\hat{\Omega}_j, \hat{\Omega}_k \,|\, (\hat{\Omega}_i\hat{\Omega}_j)(\hat{\Omega}_i\hat{\Omega}_k))$ the conditional probability of overlap of j and k given that i and j and i and k overlap. Since the two-particle overlap is simply expressed in the excluded volume by

$$P^{(2)}(\hat{\Omega}_i, \hat{\Omega}_j) = E(\hat{\Omega}_i \, . \, \hat{\Omega}_j)/V, \tag{3.2.4}$$

the problem is reduced to evaluating the conditional probability. This method of phase-space reduction was first applied by Ree and Hoover in their calculations of virial coefficients for the hard-sphere and hard disc systems [24].

The conditional probability is very suited to a calculation through Monte-Carlo with importance sampling, the procedure being as follows. Fixing particle 1 in the origin and choosing an initial configuration where particle 2 and particle 3

both overlap with particle 1, new configurations are generated by randomly moving the positions of 2 and 3 while keeping their orientations fixed. A parameter sets the maximum distance Δr over which a move is attempted. If the new configuration also has 2 and 3 overlapping with 1, the move is accepted. After each try we test for overlap of 2 and 3. After a run consisting of a suitable number of tries, the conditional overlap probability will be approximated by

$$P_c^{(3)} \simeq \frac{N_{acc}}{N_{try}} = \frac{\text{number of overlaps of 2 and 3}}{\text{number of configurations tried}}. \tag{3.2.5}$$

A measure of the accuracy of this procedure is obtained by bunching the data in a run into sub-runs and computing the root-mean-square deviation of the sub-run averages to the average over the whole run. This deviation typically shows a $1/\sqrt{N_{acc}}$ type behaviour. We implemented this procedure using the overlap-criterion for ellipsoids developed by Vieillard–Baron [25]. To obtain an accuracy of the order of 0·5 per cent we were required to make runs with $2{\cdot}5 \times 10^5$ acceptances (5×10^5 to 10^6 tries), taking about 50 seconds of computertime on a Cyber 7600 on the average. To obtain a reasonable angular resolution of $P_c^{(3)}$ would therefore be quite consuming. Consider the invariant expansion of $P_c^{(3)}$

$$P_c^{(3)}(\hat{\Omega}_1, \hat{\Omega}_2, \hat{\Omega}_3) = \sum_{\substack{l_1 l_2 l_3 \\ m_1 m_2 m_3}} p_{l_1 l_2 l_3} \begin{pmatrix} l_1 & l_2 & l_3 \\ m_1 & m_2 & m_3 \end{pmatrix} C_{l_1}^{m_1}(\hat{\Omega}_1) C_{l_2}^{m_2}(\hat{\Omega}_2) C_{l_3}^{m_3}(\hat{\Omega}_3). \tag{3.2.6}$$

We have used the standard Wigner $3-j$ symbols and modified spherical harmonics [26]. Performing an azimuthal average around an arbitrary space axis one gets

$$\tilde{P}_c^{(3)}(\theta_1, \theta_2, \theta_3) = (2\pi)^3 \sum_{l_1 l_2 l_3} p_{l_1 l_2 l_3} \begin{pmatrix} l_1 l_2 l_3 \\ 0\,0\,0 \end{pmatrix} P_{l_1}(\cos\theta_1) P_{l_2}(\cos\theta_2) P_{l_3}(\cos\theta_3). \tag{3.2.7}$$

The expansion coefficients can then be found by integration. Computing them for all values of $l_i \leqslant 2k$ requires a Gaussian integration with $(k+1)^3$ abscissas. Choosing $k = 5$ this would amount to appr. 3 hours of computertime for every ellipsoid length-to-breadth ratio considered. Trials at a value of $x = 3$ revealed that $P_c^{(3)}$ was a rather smoothly varying function of the angles involved that deviated only 20 per cent from its average over a wide range of angles. We therefore chose to approximate $P_c^{(3)}$ by its average over all particle orientations: $\bar{P}_c^{(3)}$. Notice that this approximation breaks the three-particle interchange symmetry present in the original probability $P^{(3)}$. We therefore have to resymmetrize the result

$$\begin{aligned} P^{(3)}(\hat{\Omega}_1, \hat{\Omega}_2, \hat{\Omega}_3) \cong \tfrac{1}{3}\bar{P}_c^{(3)}\{&P^{(2)}(\hat{\Omega}_1 \cdot \hat{\Omega}_2) P^{(2)}(\hat{\Omega}_1 \cdot \hat{\Omega}_3) \\ &+ P^{(2)}(\hat{\Omega}_1 \cdot \hat{\Omega}_3) P^{(2)}(\hat{\Omega}_2 \cdot \hat{\Omega}_3) + P^{(2)}(\hat{\Omega}_1 \cdot \hat{\Omega}_2) P^{(2)}(\hat{\Omega}_2 \cdot \hat{\Omega}_3)\}. \end{aligned} \tag{3.2.8}$$

By construction our approximation is exact in the isotropic phase, where only the unweighted orientational average of $P^{(3)}$ enters in the calculation of B_3.

The results for the different length-to-breadth ratios are summarized in table 1. For the cases $x = 2$ and $x = \frac{1}{2}$ the results could be compared with previous work by Freasier and Bearman [27]. Our results agree with theirs to within quoted errors. One also notes that the symmetry between systems with inverse length-to-breadth ratio, which was present at the level of the second virial coefficient, is now broken. The differences in the third virial coefficients for particles of intermediate eccentricity ($\frac{1}{3} \leqslant x \leqslant 3$) are small however ($\Delta B_3^*/B_3^* \leqslant 0{\cdot}055$).

Table 1. Table giving the values of the isotropic conditional overlap probability $\bar{P}_c^{(3)}$ and its estimated error $\Delta\bar{P}_c^{(3)}$ as well as the reduced second and third virial coefficients, $\bar{B}_2^* = B_2/v_0$ and $\bar{B}_3^* = B_3/v_0^2$ respectively.

x	$\bar{P}_c^{(3)}$	$\Delta P_c^{(3)}$	$\bar{B}_2^*$	$\bar{B}_3^*$
1·25	0·4647	0·0017	4·0534	10·1804
2·00	0·4404	0·0010	4·5385	12·0947
2·75	0·4092	0·0090	5·2107	14·8128
3·00	0·3997	0·0014	5·4537	15·8520
5·00	0·3318	0·0017	7·5520	25·2346
10·00	0·2380	0·0017	13·1913	55·2096
0·80	0·4678	0·0014	4·0534	10·2471
0·50	0·4463	0·0018	4·5385	12·2583
0·3636...	0·4297	0·0010	5·2107	15·4913
0·3333...	0·4221	0·0022	5·4537	16·7395
0·20	0·3922	0·0010	7·5520	29·8217
0·10	0·3672	0·0013	13·1913	84·1549

Another word about the validity of our approximation when we are no longer considering the isotropic case. In the limit where all the particles are perfectly aligned $P_c^{(3)}$ can be evaluated exactly. As Lebowitz and Perram have shown a global transformation of scale will map an assembly of perfectly aligned ellipsoids into a configuration of hard spheres [28]. In this case the conditional overlap probability can be easily inferred from the known result for the third virial coefficient for hard spheres. We find, regardless of the ellipsoid-length-to-breadth ratio

$$P_c^{(3)}(\text{ordered}) = \tfrac{30}{64} = 0{\cdot}46875. \tag{3.2.9}$$

Comparing this to the values in the table, and taking into account the known values of $\bar{P}_c^{(3)}$ for the limiting cases $x \to \infty$ where $\bar{P}_c^{(3)} = 0$ [2] and $x \to 0$ where $\bar{P}_c^{(3)} = 0{\cdot}3335$ [31], one infers that the approximation worsens with increasing eccentricity and also with increasing orientational order.

3.3. *The coefficients* $C_2[\psi]$ *and* $C_3[\psi]$

For our actual calculation we will need the coefficients $C_2[\psi]$ and $C_3[\psi]$ as defined in (2.12). We introduce their kernels through the following relations

$$C_2[\psi] = \int d\hat{\Omega}_1\, d\hat{\Omega}_2\, \psi(\hat{\Omega}_1)\psi(\hat{\Omega}_2)C^{(2)}(\hat{\Omega}_1 \cdot \hat{\Omega}_2), \tag{3.3.1a}$$

$$C_3[\psi] = \int d\hat{\Omega}_1\, d\hat{\Omega}_2\, d\hat{\Omega}_3\, \psi(\hat{\Omega}_1)\psi(\hat{\Omega}_2)\psi(\hat{\Omega}_3)C^{(3)}(\hat{\Omega}_1, \hat{\Omega}_2, \hat{\Omega}_3). \tag{3.3.1b}$$

Using (2.12) and our approximation as defined in (3.2.8) we find

$$C^{(2)}(\hat{\Omega}_1 \cdot \hat{\Omega}_2) = \tfrac{1}{2}E(\hat{\Omega}_1 \cdot \hat{\Omega}_2) - v_0. \tag{3.3.2a}$$

$$\begin{aligned} C^{(3)}(\hat{\Omega}_1\hat{\Omega}_2\hat{\Omega}_3) = {} & \tfrac{4}{9}\bar{P}_c^{(3)}\{C^{(2)}(\hat{\Omega}_1 \cdot \hat{\Omega}_2)C^{(2)}(\hat{\Omega}_1 \cdot \hat{\Omega}_3) \\ & + C^{(2)}(\hat{\Omega}_1 \cdot \hat{\Omega}_2)C^{(2)}(\hat{\Omega}_2 \cdot \hat{\Omega}_3) + C^{(2)}(\hat{\Omega}_1 \cdot \hat{\Omega}_3)C^{(2)}(\hat{\Omega}_2 \cdot \hat{\Omega}_3)\} \\ & - \tfrac{2}{3}v_0(1 - \tfrac{4}{3}\bar{P}_c^{(3)})\{C^{(2)}(\hat{\Omega}_1 \cdot \hat{\Omega}_2) + C^{(2)}(\hat{\Omega}_1 \cdot \hat{\Omega}_3) + C^{(2)}(\hat{\Omega}_2 \cdot \hat{\Omega}_3)\} \\ & - v_0^2(1 - \tfrac{4}{3}\bar{P}_c^{(3)}). \end{aligned} \tag{3.3.2b}$$

In the following we will work with the invariant expansions of $C^{(2)}$ and $C^{(3)}$ as given by

$$C^{(2)}(\hat{\Omega}_1 \cdot \hat{\Omega}_2) = \sum_{l=0}^{\infty} c_l P_l(\hat{\Omega}_1 \cdot \hat{\Omega}_2), \tag{3.3.3 a}$$

$$C^{(3)}(\hat{\Omega}_1, \hat{\Omega}_2, \hat{\Omega}_3) = \sum_{\substack{l_1 l_2 l_3 \\ m_1 m_2 m_3}} a_{l_1 l_2 l_3} \begin{pmatrix} l_1 & l_2 & l_3 \\ m_1 & m_2 & m_3 \end{pmatrix} C_{l_1}^{m_1}(\hat{\Omega}_1) C_{l_2}^{m_2}(\hat{\Omega}_2) C_{l_3}^{m_3}(\hat{\Omega}_3). \tag{3.3.3 b}$$

The explicit expressions for these coefficients are presented in appendix C.

4. Comparison with scaled particle theory

We are now in a position to compare the y-expansion approach as outlined in § 2 and § 3 with SPT. After briefly stating the ingredients of SPT, we discuss its application to the system of ellipsoids of revolution. The cases of one- and two-parameter scaling are considered separately.

4.1. *SPT in brief*

The central quantity of interest in SPT is the amount of reversible work done on the system to dissolve a scaled copy of the fluid particles, or equivalently to create a particle sized cavity in the fluid. The shape and size of the scaled particle can be controlled by scaling parameters $\{\lambda_j\}$, usually chosen so that $\{\lambda_j = 0\}$ represents a point particle while $\{\lambda_j = 1\}$ gives a particle identical to the system particles. If we now consider a homogeneous system, with possible long range orientational order, the following expression can be given for the work to insert a scaled particle with an orientation Ω with respect to a fixed frame into the fluid

$$-\beta W(\Omega \mid \{\lambda_j\}) = \log \left\{ \sum_{n=0}^{\infty} \frac{(-)^n}{n!} \rho^n F^{(n)}(\Omega \mid \{\lambda_j\}) \right\}. \tag{4.1.1}$$

The functions $F^{(n)}$ are related to the equilibrium n-particle distribution functions of the system through

$$F^{(n)}(\Omega \mid \{\lambda_j\}) = \left\{ \prod_{k=1}^{n} \int d\Omega_k \int d\mathbf{r}_k \psi(\Omega_k) \right\} g^{(n)}(\mathbf{r}_1 \Omega_1, \ldots, \mathbf{r}_n \Omega_n)$$

$$E(\Omega\Omega_k \mid \{\lambda_j\}). \tag{4.1.2}$$

The spatial region of integration $E(\Omega\Omega_k \mid \{\lambda_j\})$ is the excluded volume of the scaled particle with the kth system particle.

The main assumption of SPT is that $W(\Omega \mid \{\lambda_j\})$ is well approximated for all values of $\{\lambda_j\}$ by an expression of the following form:

$$W(\Omega \mid \{\lambda_j\}) = Q(\Omega \mid \{\lambda_j\}) + P v^{(0)}(\{\lambda_j\}). \tag{4.1.3}$$

Here $v^{(0)}(\{\lambda_j\})$ denotes the proper volume of the scaled particle. In three dimensions it usually is a polynomial in which the highest power of a single scaling parameter appearing is the third. $Q(\Omega \mid \{\lambda_j\})$ is a polynomial in $\{\lambda_j\}$ of degree less than that of $v^{(0)}(\{\lambda_j\})$ obtained by expanding (4.1.1) for small values of $\{\lambda_j\}$. The

approximate work-function can then be used to obtain the equation of state in several ways. We will use the one advocated by Cotter as the simplest one to achieve consistent thermodynamics [13]. In this method the work function is first averaged over all orientations. The equation of state is then obtained by integrating the Gibbs–Duhem rule

$$\frac{\partial P}{\partial \rho} = 1 + \rho \frac{\partial}{\partial \rho} \int d\Omega \psi(\Omega) W(\Omega \,|\, \{\lambda_j = 1\}). \tag{4.1.4}$$

4.2. *Two parameter scaling for ellipsoids*

We now proceed to show that SPT applied to ellipsoids will lead to an erroneous prediction of the second virial coefficients, if two parameter scaling is used. For definiteness we consider the following two scaling parameters (the argument will hold for whatever choice of independent scaling parameters):

$$b(\lambda_1) = \lambda_1 b, \quad x(\lambda_2) = \lambda_2(x - 1) + 1. \tag{4.2.1}$$

They are analogous to the ones introduced by Cotter and Martire [10]. The parameter λ_1 controls the overall size, while λ_2 scales in the length-to-breadth ratio. With this choice the scaled proper volume becomes

$$v^{(0)}(\lambda_1, \lambda_2) = \frac{4\pi}{3} b^3[(x - 1)\lambda_1^3 \lambda_2 + \lambda_1^3]. \tag{4.2.2}$$

This suggests the following form for $Q(\hat{\Omega} \,|\, \lambda_1 \lambda_2)$:

$$Q(\hat{\Omega} \,|\, \lambda_1 \lambda_2) = Q_{00} + Q_{10}\lambda_1 + Q_{01}\lambda_2 + \Omega_{20}\lambda_1^2 + Q_{21}\lambda_1^2 \lambda_2 . \tag{4.2.3}$$

The coefficients Q_{kl} are orientation and density dependent functions. Instead of determining them in full, we concentrate on their low density limit. By expanding (4.1.1) to first order in the density, we can obtain $Q(\hat{\Omega} \,|\, \lambda_1 \lambda_2)$ to this order. Insertion into (4.1.4) then yields the following expression for the second virial coefficient:

$$B_2[\psi] = \frac{1}{2}\left[v_0 + \int d\hat{\Omega}\, d\hat{\Omega}' \psi(\hat{\Omega})\psi(\hat{\Omega}')\tilde{E}(\hat{\Omega} \cdot \hat{\Omega}') \right], \tag{4.2.4}$$

with

$$\tilde{E}(\hat{\Omega}, \hat{\Omega}') = E(\hat{\Omega}\hat{\Omega}' \,|\, 00) + \frac{\partial}{\partial \lambda_1} E(\hat{\Omega}\hat{\Omega}' \,|\, 00) + \frac{\partial}{\partial \lambda_2} E(\hat{\Omega}\hat{\Omega}' \,|\, 00) + \frac{1}{2}\frac{\partial^2}{\partial \lambda_1^2} E(\hat{\Omega}\hat{\Omega}' \,|\, 00) + \frac{1}{2}\frac{\partial^3}{\partial \lambda_1^2 \, \partial \lambda_2} E(\hat{\Omega}\hat{\Omega}' \,|\, 00). \tag{4.2.5}$$

The expression for the excluded volume of a scaled ellipsoid with a reference one can be found from the expressions given by Kihara [29] for the excluded volume of two arbitrary convex bodies, combined with Isihara's [23] results on ellipsoids. It is given by

$$\begin{aligned} E(\hat{\Omega}\hat{\Omega}' \,|\, \lambda_1 \lambda_2) = {} & \tfrac{4}{3}\pi x b^3 + \tfrac{4}{3}\pi\{\lambda_2(x - 1) + 1\}\lambda_1^3 b^3 \\ & + x^2 b^3 \lambda_1 \int d\hat{n}\, \frac{(1 + ((\lambda_2(x - 1) + 1)^2 - 1)(\hat{\Omega} \cdot \hat{n})^2)^{1/2}}{(1 + (x^2 - 1)(\hat{\Omega}' \cdot \hat{n})^2)^2} \\ & + (\lambda_2(x - 1) + 1)^2 \lambda_2^2 b^3 \int d\hat{n}\, \frac{(1 + (x^2 - 1)(\hat{\Omega}' \cdot n)^2)^{1/2}}{(1 + ((\lambda_2(x - 1) + 1)^2 - 1)(\hat{\Omega} \cdot \hat{n})^2)^2} . \end{aligned} \tag{4.2.6}$$

The essential point here is the fact that $E(\hat{\Omega}\hat{\Omega}'|\lambda_1\lambda_2)$ is not polynomial in the second scaling parameter λ_2. Thus (4.2.5) will never produce the correct excluded volume minus v_0 necessary to turn (4.2.4) into an identity. In fact one obtains an approximate B_2, where the approximation is clearly dependent on the choice of scaling parameters. This defect was not noticed up to now, as this scheme has only been applied to the hard-sphero-cylinder and hard cylinder [30] cases, where the scaled excluded volume is a simple polynomial, such that (4.2.4) is indeed satisfied.

Failure to predict the correct second virial coefficient is of course unsatisfactory from a theoretical point of view. On the one hand the low density limit is not correctly reproduced. On the other hand Onsager's results for the case of extremely prolate particles, where the B_2 term becomes dominant in the virial expansion are not recovered.

4.3. *Single parameter SPT*

The problem regarding the second virial coefficient can be resolved by turning to single parameter SPT. Here the scaled particle is an isomorphic copy of the fluid particles. This approach was first applied by Lasher to the spherocylinder system [9]. Gibbons later considered its formulation for isotropic fluids of arbitrary convex hard particles [8]. In this case it is easy to show that the scaled excluded volume is given by

$$E(\hat{\Omega}_1\hat{\Omega}_2|\lambda) = (1+\lambda^3)v_0 + \lambda(1+\lambda)C^{(2)}(\hat{\Omega}_1\hat{\Omega}_2). \tag{4.3.1}$$

We recognize the previously defined kernel $C^{(2)}$ through its relation to the excluded volume (see (3.3.2 *a*). The SPT prediction for the second virial coefficient now reads

$$B_2[\psi] = \frac{1}{2}\left[v_0 + \int d\hat{\Omega}_1\, d\hat{\Omega}_2\, \psi(\hat{\Omega}_1)\psi(\hat{\Omega}_2) \times \left\{E(\hat{\Omega}_1\hat{\Omega}_2|0) + \frac{\partial}{\partial\lambda}E(\hat{\Omega}_1\hat{\Omega}_2|0) + \frac{1}{2}\frac{\partial^2}{\partial\lambda^2}E(\hat{\Omega}_1\hat{\Omega}_2|0)\right\}\right]. \tag{4.3.2}$$

Inserting (4.3.1) into (4.3.2) one immediately obtains the correct relation for B_2 (see 2.12 *a*).

One can now go through the SPT programme to obtain the equation of state. We simply give the result

$$\beta P = y + C_2[\psi]y^2 + \tilde{C}_3[\psi]y^3. \tag{4.3.3}$$

The coefficient $\tilde{C}_3[\psi]$ is given by

$$\tilde{C}_3[\psi] = \frac{1}{3}\int d\hat{\Omega}_1\, d\hat{\Omega}_2\, d\hat{\Omega}_3\, \psi(\hat{\Omega}_1)\psi(\hat{\Omega}_2)\psi(\hat{\Omega}_3)C^{(2)}(\hat{\Omega}_1 \cdot \hat{\Omega}_2)C^{(2)}(\hat{\Omega}_1 \cdot \hat{\Omega}_3). \tag{4.3.4}$$

Notice that the equation of state is of exactly the same form as the third order y-expansion. The sole difference is the coefficient $\tilde{C}_3[\psi]$. It should be compared with our approximation as given in (3.2.8). Since our results for C_3 are exact in the isotropic phase, we have carried out the comparison in that case. The results for the relative difference between the two are given in figure 1. The difference is seen to increase with increasing ellipsoid eccentricity and more marked for prolate than for oblate elipsoids.

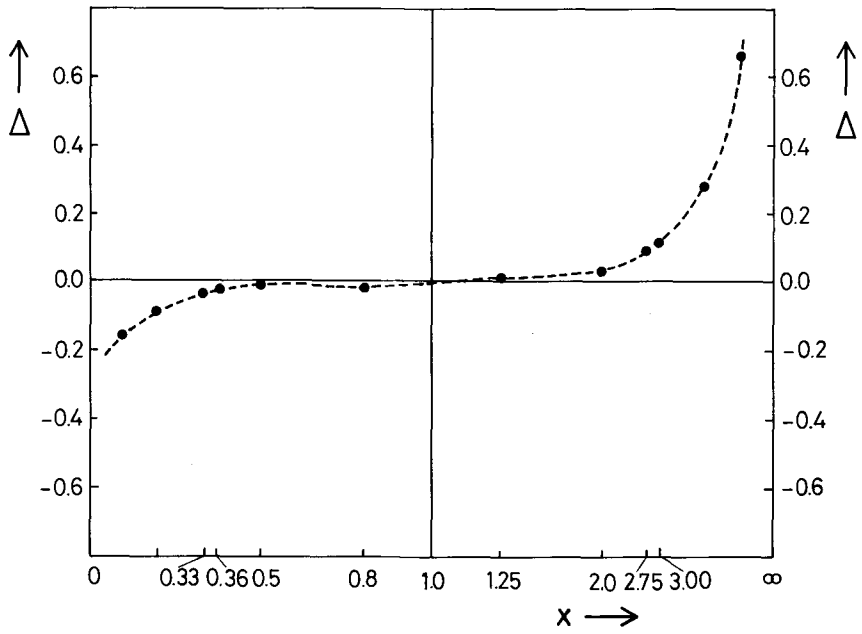

Figure 1. The relative discrepancy $\Delta = (\bar{C}_3^{\mathrm{SPT}} - \bar{C}_3)/\bar{C}_3$ of the SPT prediction for $\bar{C}_3$ and the exact result as a function of length-to-breadth ratio.

Of course there is no *a priori* reason to reject the SPT result in favour of the y-expansion. One could look on $\tilde{C}_3$ as a sort of 'renormalized' expansion coefficient, in some way effectively taking into account the influence of more particle effects. However the following comments are in order. As in the two parameter case neither the low density limit nor the Onsager limit are correctly reproduced. Concerning the latter one in fact finds that the $\tilde{C}_3$ term will dominate the C_2 term for larger eccentricities, in sharp contrast with the known result. Furthermore SPT lacks the possibility of systematic improvement, possible in the y-expansion, through the inclusion of higher order terms. In the light of these shortcomings SPT, in our opinion, compares unfavourably with the y-expansion.

5. Constructing the equation of state

To obtain the equation of state we vary the free-energy functional at a fixed number density, with respect to the orientation distribution function $\psi(\hat{\Omega})$, under the constraint that ψ has unit norm. We truncate the free-energy functional after the second order term in y, yielding

$$\frac{\beta F[\psi]}{N} = \int d\hat{\Omega}\psi(\hat{\Omega}) \ln \psi(\hat{\Omega}) - 1 - \Lambda + \ln y + yC_2[\psi] + \tfrac{1}{2}y^2 C_3[\psi]. \quad (5.1)$$

Variation with respect to ψ, while keeping the integral over ψ fixed yields the following equation:

$$\ln \psi(\hat{\Omega}) + 2y \int d\hat{\Omega}'\psi(\hat{\Omega}')C^{(2)}(\hat{\Omega} \cdot \hat{\Omega}') + \tfrac{3}{2}y^2 \int d\hat{\Omega}'\, d\hat{\Omega}''\, \psi(\hat{\Omega}')\psi(\hat{\Omega}'')C^{(3)}(\hat{\Omega}, \hat{\Omega}', \hat{\Omega}'') = \text{constant}. \quad (5.2)$$

The constant is determined from the constraint

$$\int d\hat{\Omega}\psi(\hat{\Omega}) = 1. \tag{5.3}$$

After obtaining ψ the equation of state immediately follows from (2.10). From symmetry we can restrict ourselves to unaxial distributions. Thus we can write

$$\psi(\hat{\Omega}) = \frac{1}{4\pi} S(\xi), \quad \xi = \hat{\Omega} \cdot \hat{e}_z. \tag{5.4}$$

Here ξ is direction cosine of the long axis of the ellipsoid with respect to a fixed z-axis. The distribution function $S(\xi)$ has the following properties:

$$\int_0^1 d\xi S(\xi) = 1, \quad S(\xi) = S(-\xi). \tag{5.5}$$

To be able to solve (5.2) we have to choose a representation for $S(\xi)$. We chose

$$S(\xi) = \exp\left[\sum_{l=0}^{\infty}{}' q_l P_l(\xi)\right]. \tag{5.6}$$

The prime again denotes the fact that due to the evenness of $S(\xi)$ only even terms in the expansion contribute. The advantage of this representation over a direct expansion in Legendre polynomials, lies in the fact that the positivity of $S(\xi)$ is guaranteed. Furthermore there is some numerical evidence that most realistic distribution functions can be accurately described by only a few terms in the exponent of (5.6) [31]. Inserting (5.6) into (5.2) and (5.3) and averaging out the term in $P_k(\xi)$ yields

$$q_k + 2yc_k\langle P_k\rangle + \tfrac{3}{2}y^2\sum_{l'l''} a_{kl'l''}\begin{pmatrix} k & l' & l'' \\ 0 & 0 & 0 \end{pmatrix}\langle P_{l'}\rangle\langle P_{l''}\rangle = 0, \qquad k = 1, 2, \ldots, \tag{5.7}$$

where

$$\langle P_k\rangle = \int_0^1 d\xi S(\xi)P_k(\xi) \tag{5.8}$$

and the equation describing the norm of $S(\xi)$

$$q_0 = -\ln\left[\int_0^1 d\xi \exp\left\{\sum_{l=2}^{\infty}{}' q_l P_l(\xi)\right\}\right]. \tag{5.9}$$

In practice we truncated the sum in the exponent of (5.6) after the term with $l = 10$. Then (5.7) and (5.9) become a set of five coupled equations for the coefficients q_{2k} with $k = 1, 2, 3, 4, 5$. Notice that the isotropic solution $q_k = 0$ for $k \neq 0$ exists for all values of y. It need not however be the solution with lowest free-energy. Two phase equilibria could be constructed by solving the thermodynamic equilibrium conditions:

$$\left.\begin{aligned} \mu_{\text{iso}}(y_{\text{iso}}) &= \mu_{\text{nem}}(y_{\text{nem}}, \{q_{2k}\}), \\ P_{\text{iso}}(y_{\text{iso}}) &= P_{\text{nem}}(y_{\text{nem}}, \{q_{2k}\}), \end{aligned}\right\} \tag{5.10}$$

in conjunction with (5.7) and (5.9). The additional variables here are the y-densities of the isotropic and uniaxially-ordered nematic fluid respectively.

6. Results

We will discuss the results of our calculations in two parts. The first deals with the equation of state in the isotropic phase. The second part is devoted to the results concerning the isotropic-to-nematic transition. Throughout we employ the reduced pressure and density units already defined in I

$$P^* = 8ab^2\beta P, \quad \rho^* = 8ab^2\rho. \tag{6.1}$$

6.2. *The isotropic phase*

Guided by the MC-calculation results from I we can make a direct comparison between theory and 'experiment' for the cases $x = 1{\cdot}25$; $2{\cdot}0$; $2{\cdot}75$; $3{\cdot}0$ and their inverses $x = 0{\cdot}8$; $0{\cdot}5$; $0{\cdot}3636\ldots$; $0{\cdot}333\ldots$. To obtain a meaningful comparison we constrain the y-expansion equation of state to its isotropic solution. In some of the cases considered the full y-expansion free-energy construction would predict an isotropic-to-nematic transition at a density, where the simulation still gives us an isotropic phase. This is discussed in more detail in the next section.

The results for the prolate systems are displayed in figure 2. The results for the corresponding oblate systems are not sufficiently different, neither the theoretical predictions nor the MC-results, to warrant a separate figure. On the theoretical side this is due to the relatively small difference in the third y-expansion coefficient (cf. table 1), contributing to a maximum relative pressure difference $\Delta P^*/P^* \sim 0{\cdot}06$ at $\rho^* \sim 1$ between the system with $x = 3$ and $x = 1/3$. This difference is even less for the less eccentric systems. As a measure for the quantitative agreement between the predicted equation of state and the MC-result, we take the relative difference in pressure at the point where the simulation indicates a transition to a more ordered phase. Table 2 lists these differences for the cases considered. The most extreme deviation is achieved for $x = 1/3$ where the discrepancy is of the order of 33 per cent.

The following observations can be made on the results. Most notably the third order y-expansion always overestimates the isotropic pressure. This deficiency is caused by the neglect of higher order expansion terms, that give rise to negative

Table 2. Table giving the comparison between the theory and the MC-data at the transition from the isotropic to the more ordered phase. Shown are the density at the end point of the isotropic branch ρ_I^*, and the pressure at the transition P_{MC}^* and the corresponding y-expansion result P_{y-exp}^* as well as the relative difference $\Delta = (P_{y-exp}^* - P_{MC}^*)/P_{MC}^*$.

x	ρ_I^*	P_{MC}^*	P_{y-exp}^*	Δ
1·25	0·983	14·34	15·59	0·087
2·00	1·185	46·97	54·71	0·165
2·75	1·072	30·00	37·18	0·239
3·00	0·969	18·69	23·39	0·251
0·8	0·998	15·51	16·94	0·028
0·5	1·175	45·79	52·97	0·157
0·3636...	1·040	25·69	33·59	0·308
0·3333...	0·956	17·75	23·59	0·329

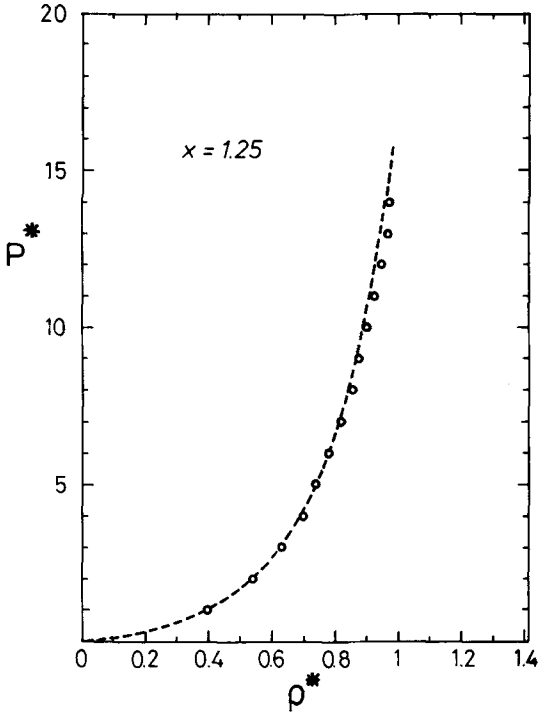
x = 1.25
P*
ρ*
20
15
10
5
0
0.2
0.4
0.6
0.8
1
1.2
1.4

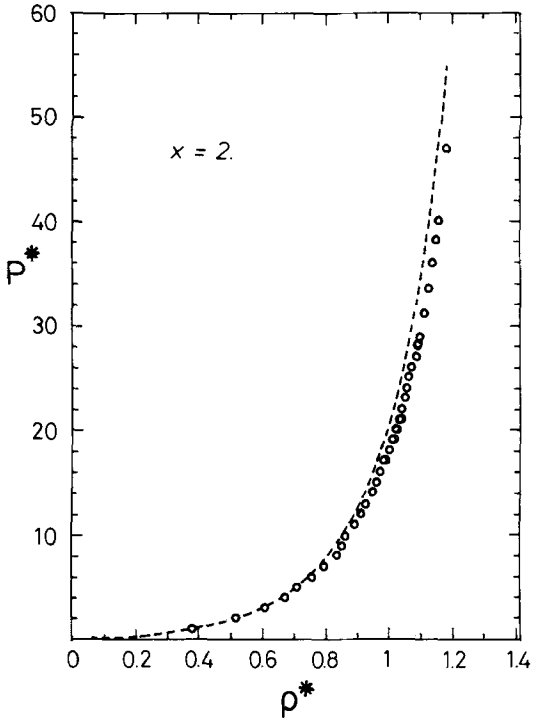
x = 2.
P*
ρ*
60
50
40
30
20
10
0
0.2
0.4
0.6
0.8
1
1.2
1.4

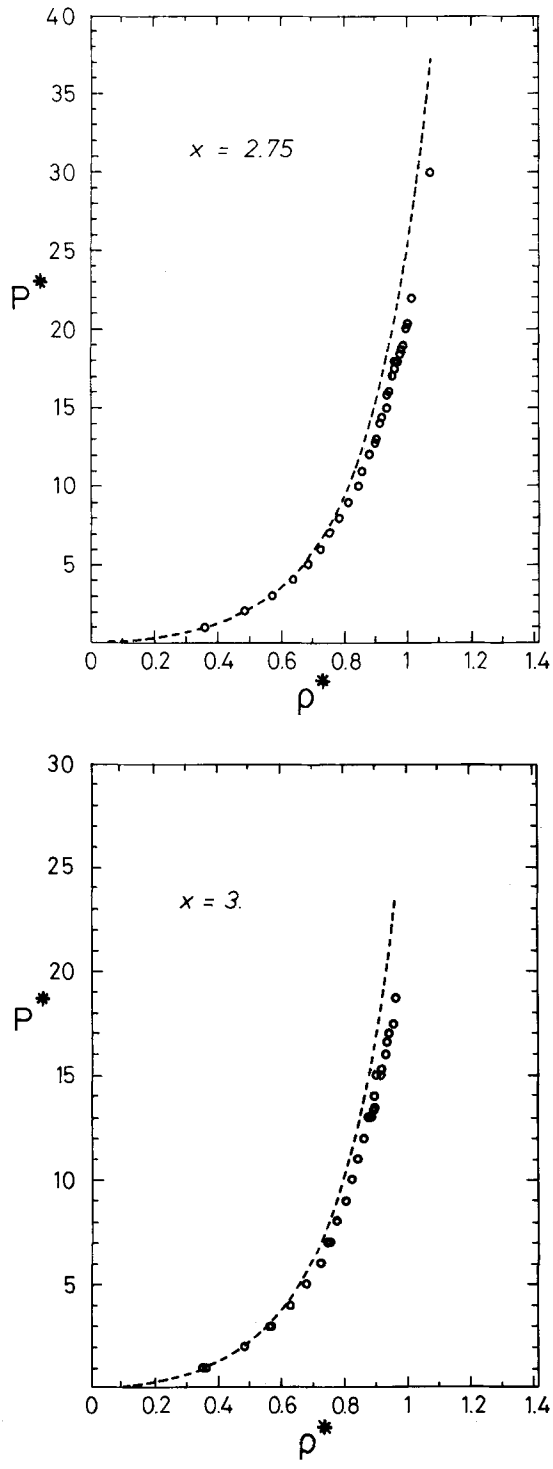

Figure 2. Equation of state in the isotropic phase predicted by the theory (dashed line) as compared to the MC-results (open circles) for several prolate ellipsoids.

contributions (cf. [17]). For the hard sphere case one indeed finds that C_4 is negative. Furthermore it is apparent that the success of the theory diminishes with increasing eccentricity. However for increasingly prolate ellipsoids the Onsager limit [2] will be reproduced by the truncated y-expansion, so that the results will tend to the exact values in that limit. For extremely oblate ellipsoids the y-expansion reduces to the ordinary virial expansion. In our approximation we would be left with a three term virial series of limited accuracy (cf. [31] for the limiting case of infinitely thin discs).

6.2. *The isotropic-to-nematic transition*

Using the technique described in § 5 the transition towards a nematic liquid crystalline phase was studied for systems with the following length-to-breadth ratios: $x = 1{\cdot}25$; $2{\cdot}0$; $2{\cdot}75$; $3{\cdot}0$, $5{\cdot}0$; $10{\cdot}0$ and their inverses. The results are summarized in table 3. Where applicable the results are compared with the simulation data. Figure 3 displays the predicted phase diagram. Since the theory can in no way account for the existence of solid phases it has the obvious deficiency of predicting stable liquid crystalline phases even if they do not exist. This is the case for $x = 1{\cdot}25$ and $x = 2{\cdot}0$ and their inverses. For the cases $x = 1{\cdot}25$ and $x = 0{\cdot}8$ the transition is even predicted to take place at an unphysical density above close packing, which in our units is reached at $\rho^* = \sqrt{2}$. For the larger eccentricities the trend seems to agree well with the simulation results. The behaviour of the order parameter $\langle P_2 \rangle_c$ is shown in figure 4. Unfortunately we were not able to obtain sufficiently accurate data on this quantity from the simulations, but the values are almost certainly lower than the ones predicted by the theory. Turning to the relative density change at the transition, we have plotted the results in figure 5. Here we see a clear overestimation with respect to the actual values.

In summary we can say that the theory predicts phase transitions that are too strong and occur at too low a density. The mechanism behind this defect is

Table 3. Table giving the results for the densities of the coexisting isotropic and nematic phases ρ^*_{iso} and ρ^*_{nem}, the critical pressure P^*_c and the jump in the order parameter at the transition $\langle P_2 \rangle_c$ as determined from the y-expansion theory. Where known, the last columns give the corresponding simulation results.

x	ρ^*_{iso}	ρ^*_{nem}	P^*_c	$\langle P_2 \rangle_c$	ρ^*_{iso}(MC)	ρ^*_{nem}(MC)	P^*_c(MC)
1·25	1·5915	1·5923	465·00	0·4379	{No nematic phase}		
2	1·0998	1·1126	34·079	0·4975			
2·75	0·8582	0·8875	12·510	0·5526	1·072	1·089	30·00
3	0·8019	0·8356	10·141	0·5677	0·969	0·988	18·69
5	0·5399	0·5945	3·9963	0·6467	—	—	—
10	0·3133	0·3712	1·7014	0·7175	—	—	—
0·8	1·5901	1·5909	466·64	0·4378	{No nematic phase}		
0·5	1·0948	1·1084	34·108	0·4967			
0·3636...	0·8462	0·8744	12·447	0·5496	1·040	1·066	25·69
0·3333...	0·7880	0·8203	10·061	0·5462	0·956	0·972	17·75
0·2	0·5111	0·5608	3·8335	0·6418	—	—	—
0·1	0·2751	0·3250	1·5160	0·7137	—	—	—

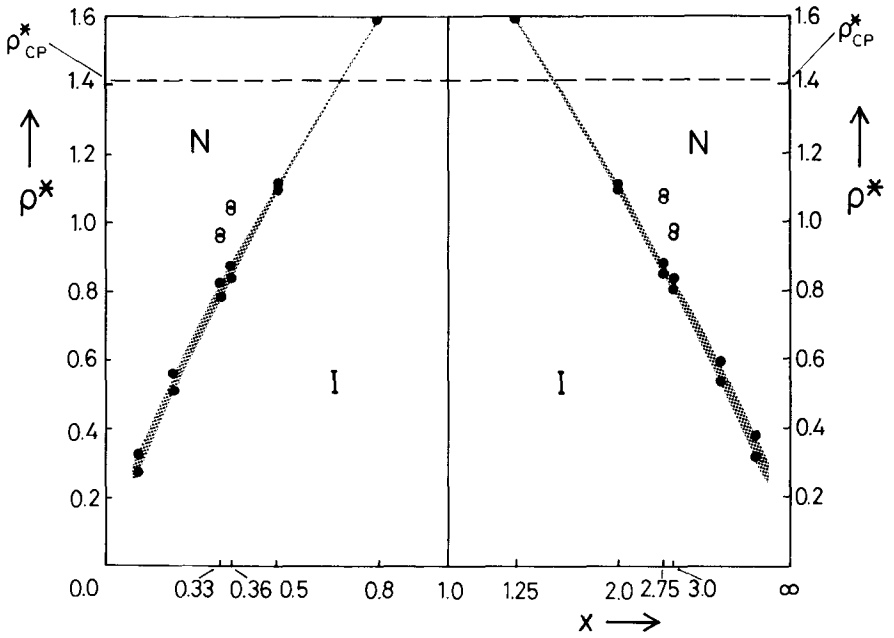

Figure 3. Predicted phase diagram. Black circles represent the calculated phase boundaries. The dotted area shows the density gap at the transition. Also shown (open circles are the MC-results for the transition for $x = 2{\cdot}75$ and $x = 3{\cdot}0$ and their inverses.

probably two-fold. First of all there is the effect of the neglect of higher order effects in the density. This will lead to an underestimation of the amount of local order, thereby exaggerating the gain in translational entropy the system can achieve by ordering. Secondly there is the influence of our approximation (3.2.8). As the values of the conditional overlap probability $P_c^{(3)}$ will tend to grow with increasing order in view of their limiting value for a totally ordered system, our

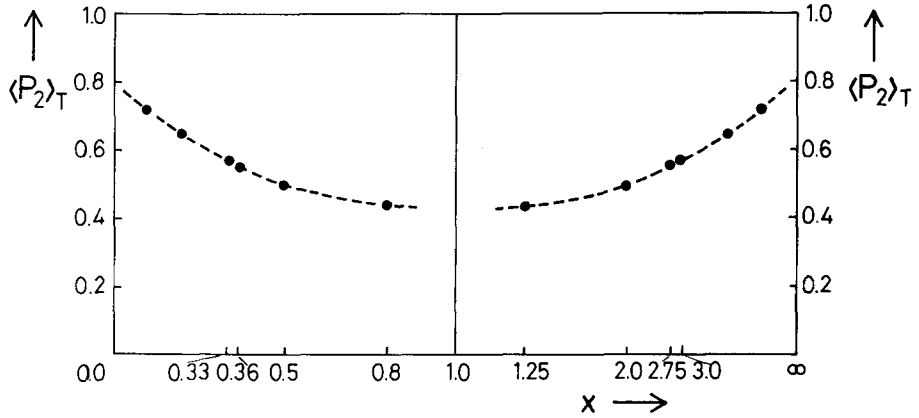

Figure 4. Jump in the order parameter $\langle P_2 \rangle_c$ at the transition as a function of length-to-breadth ratio.

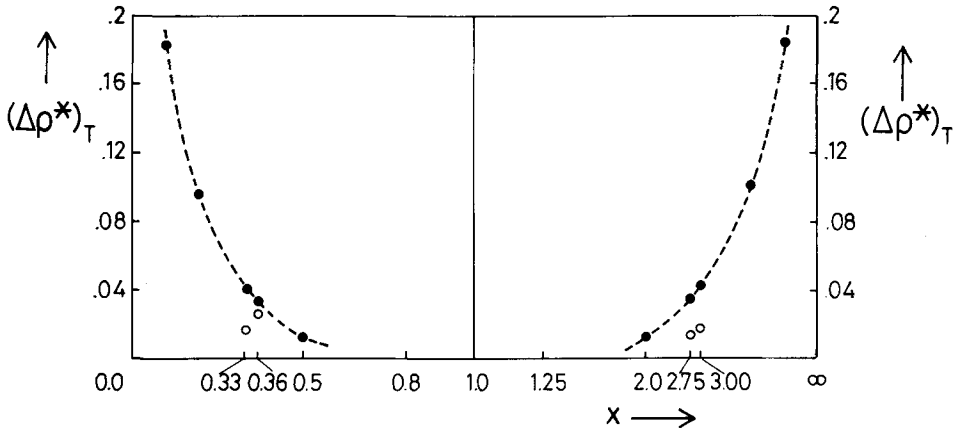

Figure 5. Relative density change $\Delta\rho^* = (\rho^*_{nem} - \rho^*_{iso})/\rho^*_{iso}$ at the transition. Also shown (open circles) the corresponding MC-data.

approximation underestimates the value of $B_3[\psi]$, and hence $C_3[\psi]$, for an ordered phase. This widens the free-energy gap between an ordered and a disordered system at the same density and so contributes to the defects we have found.

7. Concluding remarks

Our results indicate that the third order y-expansion yields a fair approximation to the equation of state in the isotropic phase for hard ellipsoids of revolution of intermediate ($1/3 \leqslant x \leqslant 3$) length-to-breadth ratio. However the agreement tends to diminish with increasing eccentricity. For the hard sphere case the third order y-expansion equation of state is identical to the result obtained from the Percus–Yevick equation, through the compressibility relation. It is unlikely that this identity persists for non-spherical particles. We would therefore not expect to obtain the same level of accuracy for the non-spherical case. This point awaits clarification however, as it has, to our knowledge, not been investigated up to now. As a feasible improvement in the isotropic regime one could consider the expansion up to higher orders, requiring the (numerical) determination of the corresponding higher order virial coefficients.

Regarding the predictions with respect to the isotropic-to-nematic transition the situation is less promising. The task of determining the kernels of higher order virial coefficients is quite formidable. Furthermore the location of the transition and its features could be strongly dependent on the order of the expansion, as is the case for the Zwanzig-gas [32]. Here the need for new techniques is felt most strongly.

We would like to thank J. P. McTague for his hospitality at the National Synchrotron Light Source in Brookhaven, where this work was started. One of us (B.M.M.) acknowledges financial support from 'Stichting FOM', which is funded by 'Nederlandse Organisatie voor Zuiver Wetenschappelijk Onderzoek (ZWO)'.

Appendix A

Following Isihara [23] we introduce the ellipsoid eccentricity as

$$\varepsilon^2 = \begin{cases} 1 - 1/x^2 & x \geqslant 1 \\ 1 - x^2 & x < 1 \end{cases}. \tag{A 1}$$

The explicit expression for the expansion coefficients a_l and b_l are then given by

$$\begin{aligned} a_{2l} &= (2\pi)^2\left(\frac{2b^3}{x}\right)F_l(\varepsilon)G_l(\varepsilon), \qquad a_{2l+1} = 0, \\ b_{2l} &= (2\pi)^2(2xb^3)H_l(\varepsilon)K_l(\varepsilon), \qquad b_{2l+1} = 0, \end{aligned} \tag{A 2}$$

where

$$\left.\begin{aligned} F_l(\varepsilon) &= \sum_{n=l}^{\infty}(-)^n\alpha_n a_{nl}\varepsilon^{2n}, \\ G_l(\varepsilon) &= \sum_{m=l}^{\infty}(-)^m\beta_m a_{ml}\varepsilon^{2m}, \\ H_l(\varepsilon) &= \sum_{p=l}^{\infty}(-)^p\alpha_p c_{pl}\varepsilon^{2p}, \\ K_l(\varepsilon) &= \sum_{q=l}^{\infty}(-)^q\beta_q c_{ql}\varepsilon^{2q}, \end{aligned}\right\} \tag{A 3}$$

with

$$\alpha_n = \frac{2}{3B(\frac{3}{2} - n,\ n+1)}, \tag{A 4a}$$

$$\beta_m = (-)^m(m+1), \tag{A 4b}$$

$$a_{nl} = (-)^l\binom{n}{l}B(n+1,\ l+\tfrac{1}{2}), \tag{A 4c}$$

$$c_{ml} = \frac{m!\,\Gamma(m+\frac{1}{2})}{(m-l)!\,\Gamma(m+l+\frac{3}{2})}. \tag{A 4d}$$

Here $B(x, y)$ is the beta-function. The expression for a_{nl} was derived from Isihara's expression

$$a_{nl} = \sum_{p=l}^{n}(-)^p\binom{n}{p}c_{pl} \tag{A 5}$$

by considering its generating function

$$A_l(z) = \sum_{n=l}^{\infty}\frac{1}{n!}a_{nl}z^n. \tag{A 6}$$

Straightforward calculation yields

$$A_l(z) = (-)^l e^z z^l\frac{\Gamma(l+\frac{1}{2})}{\Gamma(2l+\frac{3}{2})}\,{}_1F_1(l+\tfrac{1}{2},\ 2l+\tfrac{3}{2},\ -z). \tag{A 7}$$

Table 4. Values of the coefficients a_l for $l = 0, \ldots, 20$ in the case $x = 3$. One checks that in this case $\sum_{l=0}^{20}{}' \left(\frac{2l+1}{4\pi}\right) a_l/v_0 = 6{\cdot}0000003$.

l	a_l
0	$0{\cdot}11193492 \times 10^{3}$
2	$-0{\cdot}66033480 \times 10^{1}$
4	$-0{\cdot}32621916$
6	$-0{\cdot}36221317 \times 10^{-1}$
8	$-0{\cdot}52672929 \times 10^{-2}$
10	$-0{\cdot}87830100 \times 10^{-3}$
12	$-0{\cdot}15905620 \times 10^{-3}$
14	$-0{\cdot}30434746 \times 10^{-4}$
16	$-0{\cdot}60566994 \times 10^{-5}$
18	$-0{\cdot}12412219 \times 10^{-5}$
20	$-0{\cdot}26022139 \times 10^{-6}$

Inserting the integral expression for the generalized hypergeometric function

$$ {}_1F_1(a, b, z) = \frac{\Gamma(b)}{\Gamma(a)\Gamma(b-a)} \int_0^1 dt \exp(zt) t^{a-1}(1-t)^{b-a-1} \tag{A 8} $$

and differentiating with respect to z then yields the equality (A 4 c).

The expansion was checked by considering the case of parallel ellipsoids. In this case one has the obvious result

$$ E(\text{ordered}) = 8v_0 . \tag{A 9} $$

This implies that the following identities should hold:

$$ \sum_{l=0}^{\infty} \left(\frac{2l+1}{4\pi}\right) \begin{Bmatrix} a_l \\ b_l \end{Bmatrix} = 6v_0 . \tag{A 10} $$

In table 4 we give the values of a_l for the case $x = 3$, showing the typical behaviour of the coefficients (i) negative for all $l \neq 0$. (ii) quickly decreasing with increasing l.

Appendix B

In this appendix we prove the property (3.1.4); the reduced excluded volume of two ellipsoids of revolution with fixed orientations is invariant under the inversion of length-to-breadth ratio. Consider two ellipsoids u and v described by the equations

$$ \begin{aligned} F_u(\mathbf{r}) &= (\mathbf{r} - \mathbf{r}_u)^T \,.\, \mathbf{U} \,.\, (\mathbf{r} - \mathbf{r}_u) - 1 = 0, \\ F_v(\mathbf{r}) &= (\mathbf{r} - \mathbf{r}_v)^T \,.\, \mathbf{V} \,.\, (\mathbf{r} - \mathbf{r}_v) - 1 = 0. \end{aligned} \tag{B 1} $$

The matrices $\mathbf{U}$ and $\mathbf{V}$ are given by

$$ \mathbf{U} = \sum_{j=1}^{3} R_j^{-2} \hat{u}_j \otimes \hat{u}_j , \quad \mathbf{V} = \sum_{j=1}^{3} R_j^{-2} \hat{v}_j \otimes \hat{v}_j . \tag{B 2} $$

Here $\{\hat{u}_j\}_{j=1,2,3}$ and $\{\hat{v}_j\}_{j=1,2,3}$ are orthonormal vectors along the axes of symmetry of the ellipsoids. The axis lengths are given by $R_1 = R_2 = b$ and $R_3 = a = xb$, where x is the length-to-breadth ratio. The relative orientation of the ellipsoids is given by the angle θ: $\cos\theta = (\hat{u}_3 \cdot \hat{v}_3)$. If we denote by $\chi_{uv}(\mathbf{r}_{uv})$ the overlap function for ellipsoids

$$\chi_{uv}(\mathbf{r}_{uv}) = \begin{cases} 1 & \text{if } u \text{ and } v \text{ overlap,} \\ 0 & \text{if } u \text{ and } v \text{ do not overlap,} \end{cases} \tag{B 3}$$

the excluded volume of u and v is given by the following integral over the relative separation $\mathbf{r}_{uv} = \mathbf{r}_v - \mathbf{r}_u$ of u and v

$$E(u, v) = \int d\mathbf{r}_{uv}\, \chi_{uv}(\mathbf{r}_{uv}). \tag{B 4}$$

We now apply a global transformation of scale to the whole system: given by

$$\mathbf{r} = \mathbf{S} \cdot \mathbf{r}', \quad \mathbf{S} = \sum_{j=1}^{3} R_j \hat{u}_j \otimes \hat{u}_j. \tag{B 5}$$

This transformation maps u into the unit sphere u' and v into an ellipsoid v' described by the equation

$$\left.\begin{aligned} F_{v'}(\mathbf{r}') &= (\mathbf{r}' - \mathbf{r}'_{v'})^T \cdot \mathbf{V}' \cdot (\mathbf{r}' - \mathbf{r}') - 1 = 0, \\ \mathbf{V}' &= \sum_{ijk} \frac{R_i R_k}{R_j^2} (\hat{u}_i \cdot \hat{v}_j)(\hat{u}_k \cdot \hat{v}_j) \hat{u}_i \otimes \hat{u}_k \\ &\equiv \sum_{ik} V'_{ik}\, \hat{u}_i \otimes \hat{u}_k. \end{aligned}\right\} \tag{B 6}$$

The excluded volume of u' and v' is related to the original one by

$$E(u, v) = ab^2 E(u', v'), \tag{B 7}$$

where ab^2 is simply the jacobian of the transformation (B 5). Since u' is the unit sphere no angles are involved in the problem with u' and v' . $E(u', v')$ will therefore be a function of the axis-lengths of v', which are the only relevant quantities left. They can be determined from the eigenvalues of $\mathbf{V}'$. To this end we look at the characteristic polynomial of $\mathbf{V}'$. We find

$$\left.\begin{aligned} P(\lambda) &= \det(\mathbf{V}' - \lambda \mathbf{1}) \\ &= 1 - p(x)\lambda + p(x)\lambda^2 - \lambda^3, \\ p(x) &= 1 + \left(x^2 + \frac{1}{x^2}\right) + \cos^2\theta \left[2 - \left(x^2 + \frac{1}{x^2}\right)\right]. \end{aligned}\right\} \tag{B 8}$$

The symmetry under length-to-breadth ratio inversion: $x \to 1/x$ is evident. As the eigenvalues will now have the same symmetry, this property is shared by the excluded volume $E(u', v')$ itself. If we denote the hard core volume of u and v by $v_0 = (4\pi/3)ab^2$ we have from (B7) that $E^*(u, v) = [E(u, v)/v_0]$ also has the desired symmetry implying the result (3.1.4).

Appendix C

Using the results of appendix A the coefficients of $C^{(2)}$ are given by

$$c_l = \begin{cases} \frac{1}{2}a_l, & x > 1, \\ \frac{1}{2}b_l, & x < 1. \end{cases} \tag{C 1}$$

Using the addition formula

$$P_l(\hat{\Omega} \cdot \hat{\Omega}') = \sum_{m=-l}^{l} C_l^m(\hat{\Omega}) C_l^{*m}(\hat{\Omega}') \tag{C 2}$$

and the contraction formula:

$$C_l^m(\hat{\Omega}) C_{l'}^{m'}(\hat{\Omega}) = \sum_{l''m''} (2l' + 1)(-)^{m''} \begin{pmatrix} l & l' & l'' \\ m & m' & m'' \end{pmatrix} \begin{pmatrix} l & l' & l'' \\ 0 & 0 & 0 \end{pmatrix} C_{l''}^{m''}(\hat{\Omega}). \tag{C 3}$$

The coefficient $a_{l_1 l_2 l_3}$ can be expressed in c_l through

$$\begin{aligned} a_{l_1 l_2 l_3} = {} & \tfrac{4}{9}\bar{P}_c^{(3)} \begin{pmatrix} l_1 & l_2 & l_3 \\ 0 & 0 & 0 \end{pmatrix} \\ & \times \{(2l_1 + 1)c_{l_2} c_{l_3} + (2l_2 + 1)c_{l_1} c_{l_3} + (2l_3 + 1)c_{l_1} c_{l_2}\} \\ & - \tfrac{2}{3}(1 - \tfrac{4}{3}\bar{P}_c^{(3)})v_0 \\ & \times \{(2l_1 + 1)^{1/2} c_{l_1}\, \delta_{l_1 l_2}\, \delta_{l_3 0} + (2l_2 + 1)^{1/2} c_{l_2}\, \delta_{l_2 l_3}\, \delta_{l_1 0} \\ & + (2l_3 + 1)^{1/2} c_{l_3}\, \delta_{l_1 l_3}\, \delta_{l_2 0}\} \\ & - (1 - \tfrac{4}{3}\bar{P}_c^{(3)}) v_0^2\, \delta_{l_1 0}\, \delta_{l_2 0}\, \delta_{l_3 0}. \end{aligned} \tag{C 4}$$

References

[1] For a review see: Hansen, J. P., McDonald, I. R., 1976, *Theory of Simple Liquids* (Academic Press).
[2] Onsager, L., 1949, *Ann. N.Y. Acad. Sci.*, **51,** 627.
[3] Wertheim, M. S., 1963, *Phys. Rev. Lett.*, **10,** 321.
[4] Thiele, E., 1963, *J. chem. Phys.*, **39,** 474.
[5] Wertheim, M. S., 1980, *J. chem. Phys.*, **73,** 1398; 1981, *Ibid.*, **74,** 2466.
[6] Gubbins, K. E., 1980, *Chem. Phys. Lett.*, **76,** 329.
[7] Reiss, H., Frisch, H. L., and Lebowitz, J. L., 1959, *J. chem. Phys.*, **31,** 369.
[8] Gibbons, R. M., 1969, *Molec. Phys.*, **17,** 81.
[9] Lasher, G., 1970, *J. chem. Phys.*, **53,** 4141.
[10] Cotter, M. A., and Martire, D. E., 1970, *J. chem. Phys.*, **52,** 1902, 1909; 1970, *Ibid.*, **53,** 4500.
[11] Timling, K. M., 1974, *J. chem. Phys.*, **61,** 465.
[12] Cotter, M. A., 1974, *Phys. Rev.* A, **10,** 625.
[13] Cotter, M. A., 1977, *J. chem. Phys.*, **66,** 1098.
[14] Vieillard-Baron, J., 1974, *Molec. Phys.*, **28,** 809.
[15] Monson, P. A., and Rigby, M., 1978, *Chem Phys. Lett.*, **58,** 122.
[16] Nezbeda, I., and Boublik, T., 1978, *Czech. J. Phys.* B, **28,** 353.
[17] Barboy, B., and Gelbart, W. M., 1979, *J. chem. Phys.*, **71,** 3053.
[18] Barboy, B., and Gelbart, W. M., 1980, *J. statist. Phys.*, **22,** 685, 709.
[19] Nezbeda, I., Pavlicek, J., and Lubik, S., 1979, *Colln Czech. chem. Commun.*, **44,** 3555.
[20] Frenkel, D., and Mulder, B. M., 1985, *Molec. Phys.*, **55,** 1171.
[21] Morita, T., and Hiroike, K., 1960, *Prog. theor. Phys.*, **23,** 1006; 1961, *Ibid.*, **24,** 317; 1961, *Ibid.*, **25,** 537.

[22] STECKI, J., and KLOCZKOWSKI, A., 1979, *J. Phys. Coll., Paris*, **C3,** 360.
[23] ISIHARA, A., 1956, *J. chem. Phys.*, **19,** 1142.
[24] REE, F. H., and HOOVER, W. G., 1964, *J. chem. Phys.*, **40,** 939.
[25] VIEILLARD-BARON, J., 1972, *J. chem. Phys.*, **56,** 4729.
[26] BRINK, D. M., and SATCHLER, G. R., 1962, *Angular Momentum* (Oxford University Press).
[27] FREASIER, B. C., and BEARMAN, R. J., 1976, *Molec. Phys.*, **32,** 551.
[28] LEBOWITZ, J. L., and PERRAM, J. W., 1983, *Molec. Phys.*, **50,** 1207.
[29] KIHARA, T., 1953, *Rev. mod. Phys.*, **25,** 831.
[30] SAVITHVAMMA, K. L., and MADHUSUDANA, N. V., 1981, *Molec. Crystals liq. Crystals*, **74,** 243.
[31] EPPENGA, R., and FRENKEL, D., 1984, *Molec. Phys.*, **52,** 1303.
[32] ZWANZIG, R., 1963, *J. chem. Phys.*, **39,** 1714. RUNNELS, L. K., and COLVIN, C., 1970, *J. chem. Phys.*, **53,** 4219.